Carbohydrate Polymers 113 (2014) 597–606

Contents lists available at ScienceDirect

Carbohydrate Polymers

journal homepage: www.elsevier.com/locate/carbpol

Dextran-*graft*-linear poly(ethylene imine)s for gene delivery: Importance of the linking strategy

Sofia Ochrimenko[a,b,1], Antje Vollrath[b,1], Lutz Tauhardt[b], Kristian Kempe[b,2], Stephanie Schubert[a,c], Ulrich S. Schubert[b,c,**], Dagmar Fischer[a,c,*]

[a] Department of Pharmaceutical Technology, Institute of Pharmacy, Friedrich-Schiller-University Jena, Otto-Schott-Str. 41, 07745 Jena, Germany
[b] Laboratory of Organic and Macromolecular Chemistry (IOMC), Friedrich-Schiller-University Jena, Humboldtstr. 10, 07743 Jena, Germany
[c] Jena Center for Soft Matter (JCMS), Friedrich-Schiller-University Jena, Philosophenweg 7, 07743 Jena, Germany

ARTICLE INFO

Article history:
Received 21 March 2014
Received in revised form 11 July 2014
Accepted 15 July 2014
Available online 29 July 2014

Keywords:
Biocompatibility
Cationized dextran
Gene delivery
Poly(ethylene imine)
Structure-property relationship

ABSTRACT

Low molar mass linear poly(ethylene imine)s (lPEI) were grafted onto dextran *via* different synthesis routes aiming at the elucidation of structure-property relationships of dextran-*graft*-linear poly(ethylene imine) (dex-*g*-lPEI) conjugates for gene delivery applications. Beside the molar mass of well-defined lPEIs and the linker unit, also the amount of lPEI in the polymeric vectors was varied. The synthesized dextran modifications were characterized regarding their chemical structure and showed enhanced complexation and stabilization of DNA against enzymatic degradation. The transfection efficiency of dex-*g*-lPEIs was increased compared to unmodified lPEI and revealed a dependency of the used linking strategy. All complexes of DNA and dex-*g*-lPEIs were found to be nontoxic, but the synthesis route showed a strong influence on the aggregation of red blood cells. In conclusion, the linking strategy of lPEI to dextran has a significant impact on the physicochemical characteristics of DNA/polymer complexes, the biocompatibility as well as the transfection efficiency.

© 2014 Elsevier Ltd. All rights reserved.

1. Introduction

Dextran, a natural hydrophilic, biodegradable polysaccharide mainly based on α-1-6-linked D-glucose units, has been widely used in medical, pharmaceutical, and drug delivery applications (Varshosaz, 2012). More than 50 years of clinical use provided an impressive proof of its safety in parenteral and oral administration, *e.g.* as lubricant in ophthalmic solutions, creams, and ointments or as coating material for diagnostic nanoparticles(Heinze, Liebert, Heublein, & Hornig, 2006; Mehvar, 2000). Additionally, several modern drug delivery systems containing dextran are under preclinical development, for instance nanoparticles, hydrogels or microspheres (Vlugt-Wensink et al., 2007). In the field of gene therapy, series of attempts have been made to selectively modify dextran with cationic moieties such as diethylaminoethyl (Eshita et al., 2009), spermine (Abdullah et al., 2010; Azzam et al., 2002; Cohen et al., 2011), protamine (Thomas, Rekha, & Sharma, 2010b), poly(L-lysine) (Maruyama et al., 1998), poly(ethylene imine) (PEI) (Jiang & Salem, 2012; Sun et al., 2011; Sun, Xiao, Cheng, Zhang, & Zhuo, 2008a; Sun, Zhang, Cheng, Cheng, & Zhuo, 2008b; Tseng & Jong, 2003), or 2,3-epoxypropyl-trimethylammonium chloride (Thomas, Rekha, & Sharma, 2010a) in order to make them suitable as non-viral vector system. PEI was thereby one of the most favored cationic polymers applied for conjugation to dextran owing to its excellent transfection efficiency.

Several studies have evaluated dextran-*graft*-poly(ethylene imine) (dex-*g*-PEI) conjugates as promising gene delivery systems in recent years. Three different strategies for conjugation were followed:

(i) Low molar mass dextran was covalently grafted onto high molar mass branched PEIs (bPEIs) or linear PEIs (lPEIs) to decrease its cytotoxicity, to enhance the complex stability and to decrease the charge effects of salts and proteins present

* Corresponding authors at: D. Fischer Department of Pharmaceutical Technology, Institute of Pharmacy, Friedrich Schiller University Jena, Otto-Schott-Str. 41, 07745 Jena, Germany. Tel.: +49 3641 949940/+49 3641 948200; fax: +49 3641 949942/+49 3641 948202.
** Corresponding authors at: Laboratory of Organic and Macromolecular Chemistry (IOMC), Friedrich-Schiller-University Jena, Humboldtstr. 10, 07743 Jena, Germany. Tel.: +49 3641 948200; fax: +49 3641 948202.
E-mail addresses: ulrich.schubert@uni-jena.de (U.S. Schubert), dagmar.fischer@uni-jena.de (D. Fischer).
[1] These authors contributed equally.
[2] Present address: Department of Chemical and Biomolecular Engineering, The University of Melbourne, Parkville 3010, VIC, Australia.

http://dx.doi.org/10.1016/j.carbpol.2014.07.048
0144-8617/© 2014 Elsevier Ltd. All rights reserved.

in the extracellular environment as also observed for stealth polymers like poly(ethylene glycol) (Knop, Hoogenboom, Fischer, & Schubert, 2010; Petersen et al., 2002; Tseng & Jong, 2003; Tseng, Tang, & Fang, 2004). Depending on the molar mass of dextran and the degree of grafting, transfection efficiencies of dex-*g*-PEI were reported to be comparable or lower than that of the unmodified PEI. This finding was ascribed to a steric hindrance of the PEI protonation causing a decreased buffering capacity dependent on the molar mass of the dextran (Tseng, Fang, Su, & Tang, 2005).

(ii) The grafting of low molar mass bPEI onto large dextran backbones was investigated. The cytotoxicity of the conjugate was lower compared to high molar mass bPEI. In addition, the transfection could be enhanced by increasing the degree of substitution (DS) of low molar mass bPEI conjugated to dextran or increasing the N/P ratio of DNA/dextran-*g*-bPEI complexes or by using serum containing media (Jiang & Salem, 2012; Sun et al., 2008a; Sun et al., 2008b). First *in vivo* studies with pEGFP were already performed in mice using *in vivo* fluorescent imaging (Chu et al., 2013).

(iii) Dextran nanoparticles were formed by crosslinking of dextran and grafted in different extents with bPEI by reductive amination. In this way, the steric hindrance of the dextran molecules to form stable complexes of PEI and plasmid could be decreased and the transgene expression as well as the cell viability were enhanced compared to unconjugated bPEI (Tripathi, Goyal, & Gupta, 2011).

Several linking strategies have been reported to covalently bind bPEI to dextran by commonly exploiting the primary amine groups. Reductive amination of oxidized dextran with bPEI results in improved complex stability, lower cytotoxicity, and higher or comparable transfection efficiency than the respective unmodified PEI dependent on the degree of grafting (Jiang & Salem, 2012; Tseng et al., 2004). The oxidation followed by conjugation represents a convenient method to form irreversible linkages in aqueous solution, but also yields adverse products with undefined chemical structures due to the occurrence of various chain scission reactions during the oxidation reaction of dextran. In another approach, dextran was functionalized with hexamethylene diisocyanate (HMDI) for subsequent reaction with PEI (Sun et al., 2008a; Xiao et al., 2010). The HMDI linkage was found to be advantageous since the functionalization reaction could be conducted fast and effectively without addition of any catalyst and by maintaining the original dextran backbone structure. However, crosslinking is an important parameter both inter- and intramolecular, which might result in non-defined structures, higher molar masses, and undesired solution properties. The functionalization of dextran with carboxymethyl groups and the subsequent amidation might also influence the original properties significantly due to the introduction of negatively charged carboxyl groups (Sun et al., 2008b).

So far, the influence of the different linker strategies has only received little attention, but might have a significant influence on the biocompatibility, transgene expression and DNA binding characteristics. Most studies also lack in systematic analysis of polymer characteristics such as molar mass, copolymer composition, but also the purity and structure of the original polymers. To gain a better insight into the structure-property relationships, a direct comparison of the effects of various linking strategies was performed. To this end, only well-defined and in depth characterized polymers were used. In contrast to previously published studies using bPEI, linear PEI (lPEI) was chosen because it can be synthesized in a controlled manner with narrow molar mass distributions and well-defined structures such as tailored end groups (Altuntaş et al., 2012; Tauhardt et al., 2011). Consequently, no intra- and intermolecular crosslinking can be expected in contrast to bPEI. lPEI with 20 ($lPEI_{20}$) and 40 repeating units ($lPEI_{40}$) were prepared and subsequently grafted onto different dextran-precursors, namely dextran aldehyde (CHO-dex), carboxymethylated dextran (CM-dex), and 4-nitrophenyl carbonate-substituted dextran (NPC-dex). The degree of the functional groups (CHO, COOH, NPC) per anhydroglucose unit (AGU) of dextran as well as the degree of substitution (DS) and the molar mass of conjugated lPEI were varied. Finally, the influence of the linker, the DS, and the molar mass of lPEI of the various dex-*g*-PEI conjugates were examined regarding the interaction with DNA, the complex formation, and the cell- and hemocompatibility as well as transgene expression.

2. Materials and methods

See supporting information.

3. Results and discussion

3.1. Synthesis of dextran-graft-poly(ethylene imine) polymers

Well-defined, proton initiated poly(2-ethyl-2-oxazoline)s (PEtOx) were initially synthesized and subsequently hydrolyzed to lPEI under acidic conditions (Scheme S1). LPEI with a theoretical molar mass of $M_n = 860\,g\,mol^{-1}$ (20 repeating units, $lPEI_{20}$) and $1720\,g\,mol^{-1}$ (40 repeating units, $lPEI_{40}$) were obtained, which both carried an active ω-primary amine end group for the subsequent conjugation to dextran (Table S1, Scheme S1). A detailed characterization of the utilized lPEI is published elsewhere (Altuntaş et al., 2012; Tauhardt et al., 2011). To evaluate the influence of the linker unit, but also of the DS and molar mass of lPEI, various lPEIs were allowed to react with different ratios with dextran-precursors. To this end, a library of various dextran-*graft*-linear poly(ethylene imine)s (dex-*g*-lPEI), was synthesized applying different dextran-precursors and degrees of functional groups. In detail, three synthesis strategies were utilized to graft lPEI to dextran: (i) reductive amination of aldehyde functionalized dextran (CHO-dex), (ii) EDC promoted coupling of lPEI to carboxymethylated dextran (CM-dex), and (iii) carbamate formation *via* activation of dextran to 4-nitrophenyl carbonate-substituted dextran (NPC-dex) followed by reaction with lPEI (Scheme 1) (Azzam et al., 2002; Sun et al., 2008b; Vandoorne, Bruneel, Vercauteren, & Schacht, 1991). In preliminary studies (data not shown), these synthesis routes were examined to enable a straightforward reaction of the primary amino functionality of lPEI with the respective active groups introduced to dextran. It was found that the reductive amination and the EDC coupling are well-suited techniques for the synthesis of various dex-*g*-lPEI. In contrast, the carbamate formation method was not qualified because significant crosslinking occurred during reaction of 4-nitrophenyl carbonate-activated dextran with lPEI, resulting in insoluble products for higher DS values (data not shown).

3.2. Reductive amination

Pharmaceutical grade dextran from *Leuconostoc mesenteroides* ($M_w = 65{,}900\,g\,mol^{-1}$, supplier information $60{,}000\,g\,mol^{-1}$) was oxidized in a low level with potassium periodate (KIO_4). This dextran sample is frequently applied in preclinical and clinical applications (Mehvar, 2000; Sun et al., 2008b). For the oxidation, two different ratios of KIO_4 per anhydroglucose unit (AGU) (1:3 and 1:10) were chosen to react with dextran. The final degree of oxidation (degree of aldehyde groups per AGU) of the products was found to be 0.51 (**CHO-dex$_{0.5}$**) and 1.09 (**CHO-dex$_{1.0}$**), as examined by hydroxylamine chloride titration, and correlates directly to the amount of KIO_4 applied per AGU (Table S2) (Zhao & Heindel, 1991). Further investigations by size exclusion chromatography

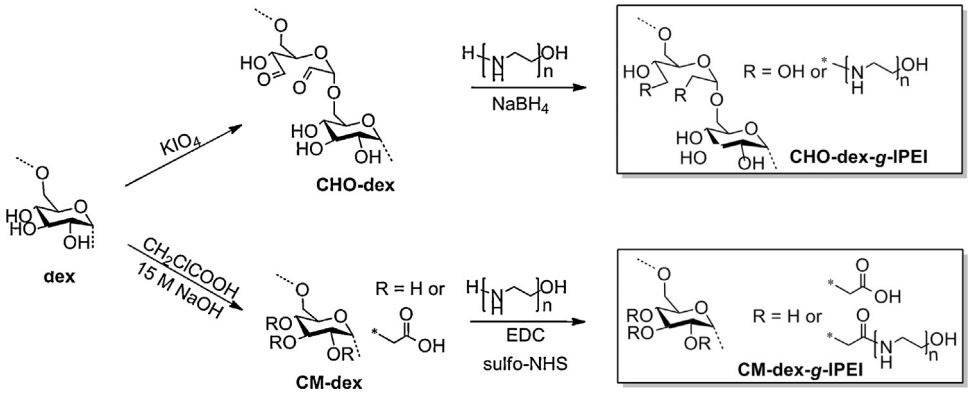

Scheme 1. Schematic representation of the functionalization of dextran by oxidation and carboxymethylation with subsequent reaction with lPEIs via reductive amination (**CHO-dex-*g*-lPEI**) and EDC coupling (**CM-dex-*g*-lPEI**), respectively.

(SEC) exhibited, as expected, a slight decrease in the molar mass due to chain degradation with increasing KIO_4-ratio (**CHO-dex$_{0.5}$**: M_w = 55,100 g mol^{-1}, **CHO-dex$_{1.1}$**: M_w = 52,500 g mol^{-1}, Table S2). The final products were further characterized by elemental analysis (EA) and ^{1}H NMR spectroscopy (Table S2, Fig. S3). In the ^{1}H NMR spectra, the signals at 3.4 ppm to 4.1 ppm can be assigned to the protons of the AGU, and the peak at 5.2 ppm to 5.3 ppm is attributed to the anomeric proton (Fig. S3). Additionally, the ^{1}H NMR spectra showed several distinctive signals in the region of 4.0 ppm to 6.0 ppm that were not present in the original dextran and give hints for different C—C bond breaking reactions as well as the formation of various hemiacetals (Jeanes & Wilham, 1950; Kent, 1949; Rankin & Jeanes, 1954).

Subsequently, the two dextran precursors were each converted with **lPEI$_{20}$** and **lPEI$_{40}$** by reductive amination in water at 60 °C (Scheme 1A). To reduce aminolysis side reactions caused by a fast conjugation rate, the pH value of the lPEI solution was adjusted to pH 6, which additionally improved the solubility of the lPEI. The DS of conjugated lPEIs per AGU was aimed to be highest 0.5, thus, the molar ratio of NH_2-lPEI to CHO was set to 1:2 for **CHO-dex$_{1.0}$** and 1:1 for **CHO-dex$_{0.5}$**. After subsequent reduction with $NaBH_4$, all dex-*g*-lPEIs (**CHO-dex-*g*-lPEIs**) were purified by extensive dialysis against water at 60 °C (for enhanced lPEI solubility), lyophilized, and investigated by ^{1}H NMR spectroscopy, EA as well as SEC measurements (Table S3, Fig. S4). In the ^{1}H NMR spectra, the signals of the CHO-dex samples are still detectable (AGU: 3.4 to 4.1 ppm; anomeric proton: 5.2 to 5.3 ppm). The additional peaks at 3.1 to 3.3 ppm correspond to the protons of the lPEI backbone and confirm the successful covalent conjugation of lPEI to CHO-dex. Various DS of lPEI per AGU were obtained (DS = 0.13 to 0.38) as calculated from the nitrogen content determined by EA (Table 1). The molar masses increase with DS from M_w = 24,000 g mol^{-1} for **CHO$_{0.5}$-dex-*g*-lPEI$_{20}$** to M_w = 36,500 g mol^{-1} for the **CHO$_{1.0}$-dex-*g*-lPEI$_{40}$** (Table S3). However, these results are not absolute values due to the fact that a dramatic rise in charge density of the polymers leads to a considerable change in the elution behavior from the column.

3.3. EDC coupling

For the second synthetic strategy, carboxylic moieties, which are able to react with the primary amino groups of the lPEIs, were introduced to the dextran backbone by carboxymethylation using monochloroacetic acid (MCA) under basic conditions (Sun et al., 2008b; Wotschadlo et al., 2009). The ratios of the reagents (dextran-AGU:MCA:NaOH = 2.2:1:1 or 1:5:10) as well as the reaction times (90 or 300 min) were altered in order to obtain different CM-dex precursors with varying DS. The lyophilized samples were characterized with regard to their content of the carboxymethyl groups according to a HPLC procedure (Heinze, Erler, Nehls, & Klemm, 1994; Liebert & Heinze, 1998). Three degrees of carboxymethyl functionalization per AGU were found, namely 0.32 (**CM$_{0.3}$-dex**), 0.54 (**CM$_{0.5}$-dex**), and 1.60 (**CM$_{1.6}$-dex**) (Table S4). The ^{1}H NMR spectra (600 MHz, D_2O) showed the expected methylene peak of the carboxymethyl group in the CM-dex at 4.1 to 4.3 ppm, and the proton signals of the AGU (3.4 to 4.1 ppm) as well as the anomeric proton peak at 5.2 to 5.3 ppm (Fig. S5). SEC data revealed increasing molar masses with increasing attachment of the carboxymethyl groups, ranging from M_w = 51,100 g mol^{-1} (**CM$_{0.3}$-dex**) up to 60,100 g mol^{-1} (**CM$_{1.6}$-dex**, Table S4).

The subsequent grafting of lPEI$_{20}$ and lPEI$_{40}$ to the various CM-dex samples was performed in water in the presence of *N*-hydroxysulfosuccinimide (sulfo-NHS) and 1-ethyl-3-(3-dimethylaminopropyl)-carbodiimide (EDC) (Sun et al., 2008b). Both **CM-dex$_{0.3}$** and **CM-dex$_{0.5}$** were allowed to react with a slight excess of lPEI (COOH:NH_2 = 1:1.2), whereas the COOH:NH_2 ratio was reduced to 3:1 for **CM-dex$_{1.6}$**. After extensive purification and lyophilization, the products (**CM-dex-*g*-lPEIs**) were characterized by ^{1}H NMR spectroscopy, SEC, and EA (Table S5). The chemical shifts of the protons of the lPEI backbone are detected at 3.1 to 3.3 ppm confirming the successful binding of the lPEIs to the CM-dextrans (Table S6) (Park et al., 2005; Sun et al., 2008b). The resulting DS of lPEI per AGU was again calculated from the nitrogen content obtained by EA and found to be in the range of 0.06 to 0.18 (Table 1). Furthermore, SEC analysis also revealed an increase of molar mass due to attachment of the lPEI to the CM-dex.

By comparing the strategies applied for the grafting of lPEI to dextran, it is apparent that both ways enabled the synthesis of various dex-*g*-lPEIs with different DS of lPEI in a straightforward manner. Although the reductive amination method reached considerably higher DS values, this technique has the drawback that the required oxidization of dextran led to ring opening reactions of the glucose, chain degradation, and other adverse side-reactions, which resulted in hardly predictable chemical structures and biophysicochemical characteristics. In contrast, during dextran activation *via* carboxymethylation the glucose units of the dextran kept their ring structure and no chain degradation occurred. However, dex-*g*-lPEIs prepared by EDC coupling additionally contained carboxylic acid functionalities (COOH) in the dextran backbone, which resulted in polyelectrolyte structures including both cationic and anionic charges that might influence the physicochemical and the biological properties as well.

3.4. Binding and protection of DNA

Nanoassemblies can be formed spontaneously by masking the anionic charge of the DNA based on electrostatic interactions

Table 1
Overview about the DS and nitrogen content of all synthesized dex-*g*-lPEI samples.

dex-*g*-lPEIs	CHO/COOH: NH_2 [mol]	DS [lPEI/AGU]	N [%]	Cationic charge/$M_{Monomer}$[a]	Anionic charge/$M_{Monomer}$[b]
Reductive amination (**CHO-dex-*g*-lPEI**)					
$CHO_{0.5}$-dex-*g*-$lPEI_{20}$	1:0.5	0.18	15.78	0.0114	–
$CHO_{0.5}$-dex-*g*-$lPEI_{40}$	1:0.5	0.13	19.12	0.0135	–
$CHO_{1.0}$-dex-*g*-$lPEI_{20}$	1:0.5	0.38	21.45	0.0156	–
$CHO_{1.0}$-dex-*g*-$lPEI_{40}$	1:0.5	0.19	21.73	0.0156	–
EDC coupling (**CM-dex-*g*-lPEI**)					
$CM_{0.3}$-dex-*g*-$lPEI_{20}$	1:1.2	0.06	6.73	0.0052	0.0013
$CM_{0.3}$-dex-*g*-$lPEI_{40}$	1:1.2	0.07	12.80	0.0093	0.0010
$CM_{0.5}$-dex-*g*-$lPEI_{20}$	1:1.2	0.07	7.96	0.0056	0.0020
$CM_{0.5}$-dex-*g*-$lPEI_{40}$	1:1.2	0.10	14.83	0.0110	0.0014
$CM_{1.6}$-dex-*g*-$lPEI_{20}$	3:1	0.11	8.16	0.0063	0.0046
$CM_{1.6}$-dex-*g*-$lPEI_{40}$	3:1	0.18	18.38	0.0127	0.0028

[a] Calculated cationic charge/molar mass of monomer unit.
[b] Calculated anionic charge/molar mass of monomer unit.

between the cationic carrier material and the anionic DNA. Complexes of lPEI modified dextran were formed with herring testes DNA as model DNA (Fischer, Dautzenberg, Kunath, & Kissel, 2004) applying different N/P ratios (0.5 to 40) and analyzed by agarose gel electrophoresis (Fig. S7 for N/P 0.5–10, for N/P ratio >10 to 40 data not shown). The complex parameters (N/P ratio) as well as the polymer characteristics (molar mass lPEI, DS and type of linker technology) were tested in a systematically modified way as they were expected to influence the interaction with DNA.

Depending on the N/P ratio, all cationic dextrans spontaneously formed interpolyelectrolyte complexes with the DNA as a result of cooperative electrostatic interactions. With increasing cationic dextran concentration, the amount of DNA migrating into the gel decreased indicating that the complexes were larger in size and/or less negatively charged than free DNA. It was explored that all **CHO-dex-*g*-lPEIs** fully complexed herring testes DNA already at an N/P ratio of 1 (Fig. S7) indicating charge balance. The complexation was found to be slightly increased with higher molar mass of lPEI coupled to CHO-dex. Other studies also showed that an increase of the molar mass of bPEI resulted in a higher binding capacity independent of the degree of grafting (Jiang & Salem, 2012). For comparison, both linear PEIs (20 and 40 monomers) also fully retarded the DNA at a N/P ratio 1 (Lungwitz, Breunig, Liebl, Blunk, & Goepferich, 2008). Furthermore, CM-dex-*g*-lPEIs were found to completely retard DNA migration into the gel at an N/P ratio firstly at 2, which indicates a weaker complexation ability compared to free lPEI and **CHO-dex-*g*-lPEI** samples. This may be attributed to the presence of the anionic charges that could interfere with lPEI and decrease the interaction with DNA. This assumption is supported by polymer **$CM_{1.6}$-dex-*g*-$lPEI_{20}$**, which contained the highest number of anionic charges and demonstrated the lowest interaction with DNA with a total complexation earliest at N/P ratio 5. The negative "charge effect" on DNA binding can be balanced by a higher DS and molar mass of lPEI grafted on the CM-dex backbone as demonstrated for sample **$CM_{1.6}$-dex-*g*-$lPEI_{40}$** (complexation at N/P ratio 1). A slight trend to higher compaction with increasing molar mass of lPEI can be found as already observed for dextran copolymers with bPEI (Sun et al., 2008b).

Compaction of plasmid DNA (pDNA) by cationized dextrans should substantially hinder the access of enzymes to the pDNA by physical or electrostatic barriers and, thus, increase the stability (Tripathi et al., 2011). To study the integrity of pDNA after enzymatic treatment by gel electrophoresis (Fig. 1), pDNA/cationized dextran complexes of different N/P ratios were treated with DNase I for 45 min. After inactivation of the enzyme by heating and release of the plasmid by dissociation of the complex using dextran sulfate, free pDNA was detected on agarose gels. Intact plasmid revealed two major fluorescent bands corresponding to the supercoiled and open circular form (Fig. 1a–c, lane 1, "untreated"). Free plasmid

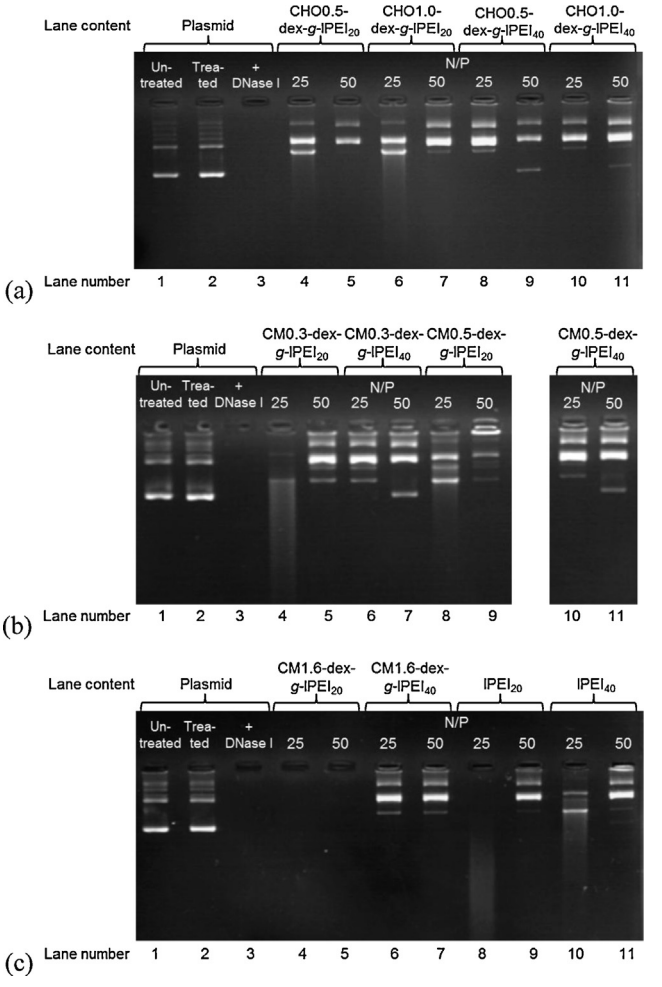

Fig. 1. Stability of dex-*g*-lPEI/plasmid complexes against enzymatic degradation (DNase I, 37 °C, 45 min) at N/P ratio 25 and 50: (a) C; (b) and (c) dex-*g*-lPEIs by EDC-coupling, (c) lPEIs. Controls: lane 1: untreated free plasmid; lane 2: free plasmid treated in the same way as complexes but without enzyme; lane 3: free plasmid treated with enzyme.

was rapidly degraded after DNase I incubation at 37 °C already after 5 min (data not shown). Thus, the characteristic bands disappeared due to degradation to lower molar mass products (Fig. 1a–c, lane 3, "DNase I"). Plasmid treated by the same procedure but without enzyme remained stable and served as control to exclude nonspecific degradation (Fig. 1a–c, lane 2, "treated").

Since in the binding studies a high N/P ratio, high molar lPEI mass and DS as well as a low number of COOH residues were identified

as parameters for an efficient interaction with DNA, they were suggested to correlate with a high enzymatic stability of the complexes. Although a full pDNA complexation by cationic dextrans already occurred at low N/P ratios, higher N/P ratios were selected for physicochemical analysis according to later transfection results. The results of the stability assay indicated that the efficiency to stabilize DNA was increased with increasing N/P ratio, higher molar masses of lPEI, and DS with lPEI independent of the type of linker. For free lPEI, a molar mass dependent interaction with pDNA could be observed (Fig. 1c, lanes 8 and 10). The higher the molar mass of free lPEI, the more efficient was the stabilizing effect of the complex. This effect could also be observed for the dex-*g*-lPEIs and was more pronounced for these than for the free lPEI. In particular, at N/P ratio 25 of dex-*g*-lPEI the stability increased with higher molar mass, which might be related to the increase in charge density within the macromolecules.

For **CHO-dex-*g*-lPEIs**, the stabilization effect was most obvious. **CHO-dex-*g*-lPEI$_{20}$** polymers revealed at N/P ratio 25 a different pattern of DNA bands compared to the **CHO-dex-*g*-lPEI$_{40}$** complexes. Changes in the topology of the plasmids are common as reported in many other studies (Fischer et al., 2004; Gebhart et al., 2002). **CHO$_{0.5}$-dex-*g*-lPEI$_{40}$** and **CHO$_{0.1}$-dex-*g*-lPEI$_{40}$** protected the plasmid better than their lPEI$_{20}$ counterparts, since at N/P ratio 25 no degradation product was visible and just a weak fluorescent band between the expected supercoiled and the open circular band appeared (Fig. 1a lanes 8 and 10). At N/P ratio 50 for both conjugates even a low fluorescent supercoiled plasmid band is still visible (Fig. 1a, lanes 9 and 11).

Likewise all **CM-dex-*g*-lPEI$_{20}$** conjugates were not able to protect the pDNA as good as their lPEI$_{40}$ counterparts. **CM$_{0.3}$-dex-*g*-lPEI$_{20}$** with the lowest DS of lPEI demonstrated at N/P ratio 25 a high plasmid damaging effect. In contrast, for **CM$_{0.3}$-dex-*g*-lPEI$_{40}$** and **CM$_{0.5}$-dex-*g*-lPEI$_{40}$**, a certain amount of supercoiled plasmid could be conserved. In accordance with the low DNA binding efficiency described above, **CM$_{1.6}$-dex-*g*-lPEI$_{20}$** was not able to stabilize plasmid DNA even at N/P ratio 50.

In summary, it could be demonstrated that improved binding and protection of DNA is basically reached with increased N/P ratio. Furthermore, the higher the molar mass of lPEI and DS with lPEIs the better the stabilization of pDNA by the conjugates due to the increase of positive charge. Thus, it is not surprising that in contrast to the **CHO-dex-*g*-lPEIs**, the **CM-dex-*g*-lPEIs** showed weaker DNA binding and less stabilization characteristics. Theses polymers are characterized by lower DS with lPEI and also by negative charges originating from the carboxymethyl (CM) functionalities within the polymer backbone that might decrease the interaction with negatively charged pDNA due to electrostatic repulsion.

3.5. Size and zeta potential of complexes

The efficiency of the dex-*g*-lPEI-mediated cellular DNA delivery will also be determined by the size and the surface charge of the complexes formed. A positive surface charge represents a prerequisite to stabilize the included nucleic acid against enzymatic degradation in small sized complexes, which are able to interact with the negatively charged cell membrane for an effective endocytosis into cellular compartments (Grund, Bauer, & Fischer, 2011). Complexes were prepared with two different N/P ratios (25 and 50) in bidistilled water to avoid any influence of the ionic strength of the solvent and were studied by light scattering with regard to the final size and surface charge. Based on the electrophoresis experiments, it was hypothesized that (i) all copolymers should be able to form small, positively charged nanoassemblies with DNA with (ii) **CHO-dex-*g*-lPEIs** being more effective than **CM-dex-*g*-lPEIs**.

In detail, all dex-*g*-lPEI/pDNA assemblies revealed sizes in the range of 70 to 113 nm with monomodal size distributions

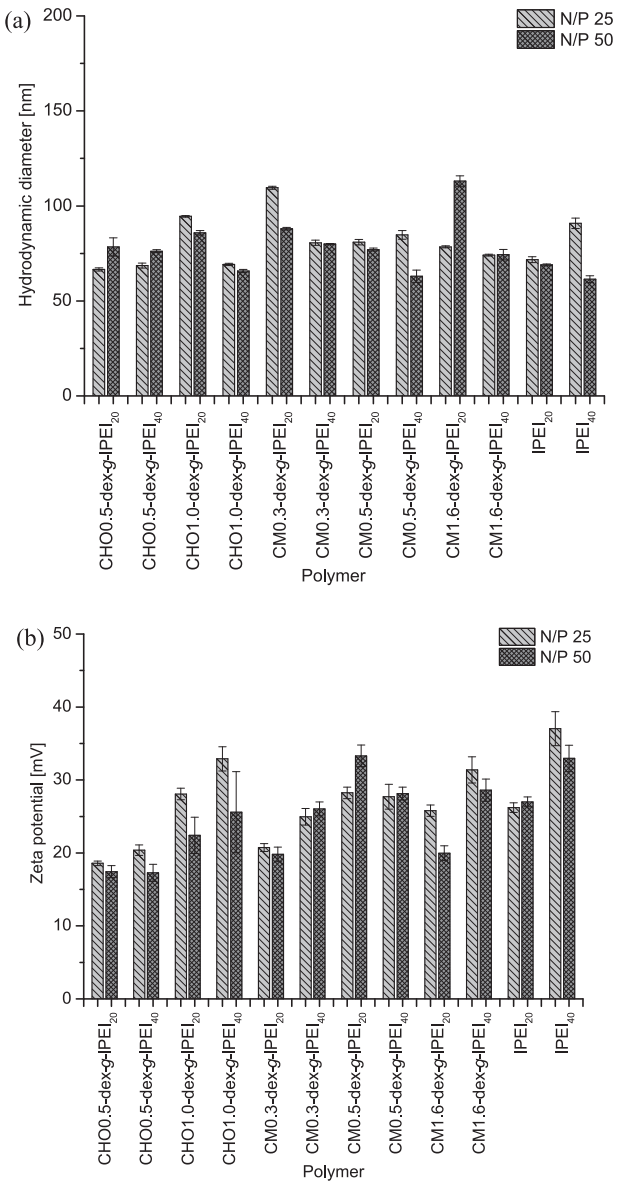

Fig. 2. (a) Hydrodynamic diameter and (b) zeta potential of dex-*g*-lPEI and lPEI complexes with plasmid DNA at N/P ratio 25 and 50 measured in water. Results are shown as mean of six measurements ± SD.

(polydispersity indices (PDI) 0.13 to 0.31, data not shown), which were comparable to the sizes obtained for the DNA complexes with lPEI$_{20}$ and lPEI$_{40}$ (Fig. 2a). Since an excess of polymer was used, no major differences could be observed between N/P ratio 25 and 50. For polymer **CM$_{1.6}$-dex-*g*-lPEI$_{20}$**, a relatively high hydrodynamic diameter of 113 nm was measured at N/P ratio 50. The insufficient DNA binding and stabilization of DNA by **CM$_{1.6}$-dex-*g*-lPEI$_{20}$** correlates with a lower DNA compaction and, consequently, a larger complex size. A similar trend was observed for **CM$_{0.3}$-dex-*g*-lPEI$_{20}$** at N/P ratio 25 (hydrodynamic diameter 110 nm). All complexes were positively charged with zeta potentials between +17 and +37 mV with comparable results for N/P ratios 25 and 50 due to the excess of the cationic component (Fig. 2b).

Additionally, complexes were prepared in 50 mM NaCl solution at pH 7.4 (data not shown). All complexes of **CHO-dex-*g*-lPEIs** prepared with N/P ratio 25 aggregated immediately. In contrast, by trend smaller sized complexes were obtained at N/P ratio 50 with diameters of about 170 to 320 nm due a more intense compaction of the plasmid by the modified dextrans, but again with a tendency to

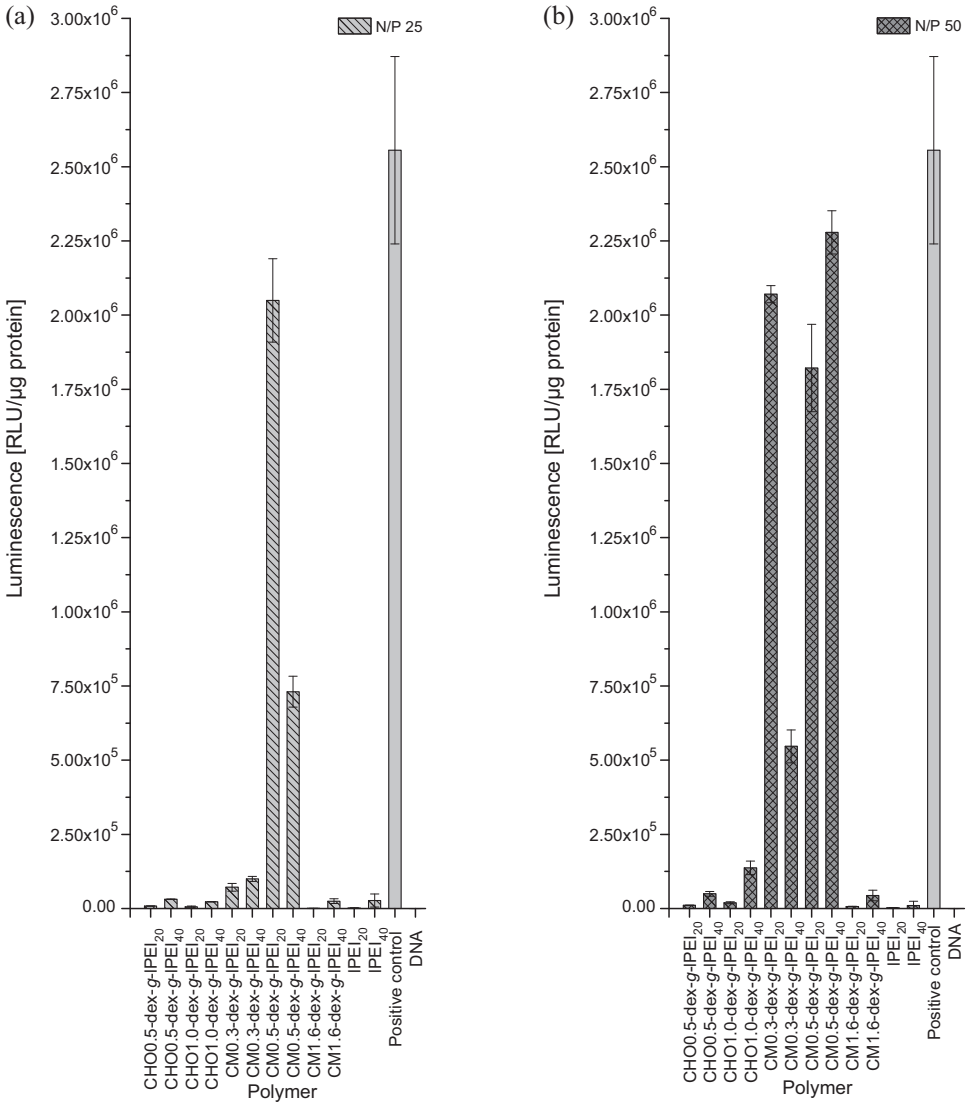

Fig. 3. Transfection efficiency of dex-*g*-lPEIs and free lPEIs complexed with plasmid pGL3 at (a) N/P ratio 25 and (b) N/P ratio 50 in CHO-K1 cells determined by luciferase assay; in comparison to the positive control 2.5 kDa lPEI at N/P ratio 25 and naked plasmid (DNA).

slowly agglomerate over time. Measurements of complexes of the CM-dex-*g*-lPEIs with pDNA in 50 mM NaCl did not lead to evaluable results due to strong aggregation, forming complexes larger than 1 μm with multimodal size distributions.

It is known that the complex formation can be strongly influenced by the medium used for preparation, since complexation is driven by electrostatic forces (van Gaal et al., 2011). Usually, the higher the ionic strength of the media the higher the impact on the complexation and the resulting complex size (Rinkenauer et al., 2013). 150 mM NaCl as iso-osmotic solution is often used for transfections, but can lead to a fast complex aggregation (Petersen et al., 2002). To reveal relevant information about the complex size for product characterization, many authors described therefore useful measurements under salt-free conditions (Cavallaro et al., 2008; Ogris, Brunner, Schuller, Kircheis, & Wagner, 1999; Ogris et al., 2003). Measurements of complexes in cell culture medium and serum supplemented cell culture medium are often misleading, since the proteins itself prevent a proper characterization by DLS. Several authors have mentioned this effect, and formation of complexes and their measurements under low salt conditions have been therefore widely described (van Gaal et al., 2011). Furthermore, in serum containing media the process of aggregation could often be avoided due to the stabilization of the complexes by the formation of a surrounding protein corona. For transfection experiments it has to be taken into consideration that possible aggregation is a time-dependent process. Consequently, complexes were freshly prepared before each biological experiment and used within 10 min. Ogris et al. (1998) hypothesized that the transfection efficacy *in vitro* might increase with larger complex sizes due to their faster sedimentation. Although we also observed aggregation for the pDNA complexes prepared from **CHO-dex-*g*-lPEIs**, they revealed a decrease in complex size demonstrating a positive impact of dextran on the complex formation in comparison to free $lPEI_{20/40}$.

However, the influence of complex aggregation on transfection, cytotoxicity and hemolysis results was not in the focus of this study and therefore, not further addressed. For future studies, a low ionic strength medium supplemented *e.g.* with glucose at iso-osmotic concentrations might be beneficial since it tolerates the characterization as well as the transfection (van Gaal et al., 2011).

3.6. Transfection mediated by pDNA/dex-g-lPEI complexes

CHO-K1 cells were transfected with complexes of the cationized dextrans and the plasmid pGL3 at different N/P ratios for 4 h. Based on preliminary experiments, N/P ratios 25 and 50 were found to be suitable for the following experiments. Luciferase expression was presented by normalizing the measured relative light units (RLU) to the total protein mass of the cells per culture well. For all tested samples, cytotoxicity-related effects as the reason for the declining transfection efficiencies were unlikely, since the protein concentrations in cell lysates (an indicator for cell growth, determined by a BCA assay) were very similar (data not shown). Free plasmid itself revealed only a limited ability to transfect cells. Unmodified dextran was tested in concentrations up to 25 $\mu g\,\mu g^{-1}$ pGL3 plasmid in a preliminary study and failed to produce any detectable level of transgene expression (data not shown). Also $lPEI_{20}$ and $lPEI_{40}$, were characterized by a low transgene expression.

The transfection experiments for the copolymers were designed to evaluate the importance of the structural polymer characteristics identified above, for the delivery of genes *in vitro*. Besides increasing N/P ratios, especially molar mass of lPEI and DS with lPEIs leading to smaller and more stable complexes, were found to be important factors for efficient DNA transfer. Furthermore, the influence of the carboxy groups of the **CM-dex-*g*-lPEIs**, which seemed to cause reduced interactions with DNA, on cellular processing of DNA has to be elucidated.

Interestingly, the transfection efficiency obtained for the **CHO-dex-*g*-lPEIs** was only slightly higher than for the corresponding free lPEIs, but cationized dextrans with negatively charged groups, prepared by EDC coupling, demonstrated a high activity (Fig. 3). For **CM-dex-*g*-lPEIs**, the transgene expression increased with higher molar mass of the lPEIs and N/P ratio, as already expected from the available physicochemical characterization data. For the **CM-dex-*g*-lPEIs**, the transfection rate increased in the range **$CM_{0.3}$-dex-*g*-$lPEI_{20}$**, **$CM_{0.3}$-dex-*g*-$lPEI_{40}$**, **$CM_{0.5}$-dex-*g*-$lPEI_{20}$** at N/P ratio 25, whereas for **$CM_{0.5}$-dex-*g*-$lPEI_{40}$** a decrease could be observed (Fig. 3a). It has to be highlighted that **$CM_{0.3}$-dex-*g*-$lPEI_{20}$**, **$CM_{0.5}$-dex-*g*-$lPEI_{20}$** and **$CM_{0.5}$-dex-*g*-$lPEI_{40}$** at N/P ratio 50 (1.8 to 2.3×10^6 RLU μg^{-1} protein, Fig. 3b) showed transfection efficiencies comparable to that of a commercially available linear 2,500 g mol^{-1} lPEI at N/P ratio 25 (2.55×10^6 RLU μg^{-1} protein, Fig. 3b). A similar effect could be observed earlier for CM-dex-PEIs (Sun et al., 2008b). **$CM_{0.3}$-dex-*g*-$lPEI_{40}$** and **$CM_{0.5}$-dex-*g*-$lPEI_{40}$** were expected to induce higher transfection rates than **$CM_{0.3}$-dex-*g*-$lPEI_{20}$** and **$CM_{0.5}$-dex-*g*-$lPEI_{20}$**, as it is known from the higher molar mass dex-*g*-bPEI conjugates(Jiang & Salem, 2012) and was also observed for the **CHO-dex-*g*-lPEIs**. However, a contrary effect was revealed for **$CM_{0.5}$-dex-*g*-$lPEI_{40}$** at N/P ratio 25 and **$CM_{0.3}$-dex-*g*-$lPEI_{40}$** at N/P ratio 50, since an approximately 1/3 lower transfection compared to their $lPEI_{20}$ counterparts was found. This is ascribed to stronger interactions between the longer lPEI chain with COOH groups of the CM-dex than with the pDNA.

In conclusion, **$CM_{0.5}$-dex-*g*-$lPEI_{20}$** provides the best gene delivery properties in this study at both N/P ratios, what might be related to the ratio of cationic charges to anionic charges per monomer (Table 1). Additionally, the low efficiency of the **CHO-dex-*g*-lPEIs** may be attributed to the higher DNA complexation efficiency of the polymer and, therefore, lower ability to release pDNA from the complexes compared to the polymers of the **CM-dex-*g*-lPEIs** as shown by the electrophoresis assays. Dissociation of DNA from the complexes is one of the critical steps in the biological process, since only released and intact DNA can be transcribed. The observed trends are in accordance with the results of the physicochemical experiments: As uptake of complexes into cells imposes certain size and stability requirements on the endocytosed material, it is necessary for a successful gene transfer that the cation in polyplexes not only binds DNA, but also compacts it. Since the condensation of DNA is also known to protect the genetic material from enzymatic degradation (Godbey, Barry, Saggau, Wu, & Mikos, 2000), the decrease of transfection ability of the complexes formed by polymers **$CM_{1.6}$-dex-*g*-$lPEI_{20}$** and **$CM_{1.6}$-dex-*g*-$lPEI_{40}$** may result from the insufficient interactions with pDNA based on the highest number of anionic charges.

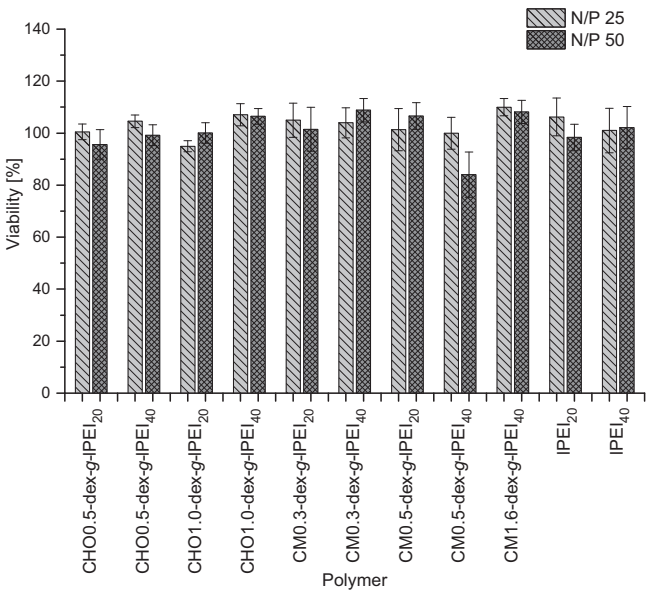

Fig. 4. Viability of L929 mouse fibroblasts treated with dex-*g*-lPEI/DNA and lPEI/DNA complexes at N/P ratio 25 and 50 for 24 h, determined by MTT assay. Complexes were formed with herring testes DNA as model DNA. Results are shown as mean of seven values ± SD.

3.7. In vitro biocompatibility testing

Biocompatibility testing has been performed with respect to cyto- and hemotoxicity. The *in vitro* cytotoxicity of the non-viral vectors was evaluated by the 3-(4,5-dimethylthiazol-2-yl)-2,5-diphenyltetrazolium bromide (MTT) assay representing the metabolic activity of cells (Fig. 4). The same conditions as in the transfection experiments were used. Independent of the N/P ratio, complexes with the two lPEIs did not cause any cytotoxic effect, which is supported by results from earlier studies demonstrating the low cytotoxicity of complexes formed with low molar mass lPEIs (Breunig et al., 2005; Thomas, Ge, Lu, Chen, & Klibanov, 2005; Yu et al., 2009). Taking the DIN ISO 10993-5 guideline (2009) into consideration which defines a reduction of cell viability lower than 70% as nontoxic, all tested dex-*g*-lPEI/DNA complexes were found to be highly compatible (84 to 110%) at N/P ratios 25 and 50. The compatibility was thereby independent of the linker technique, the DS and the selected N/P ratios (Fig. 4). For comparison, the positive control thiomersal solution (0.02%) reduced the mean cell viability to 0.6% (data not shown). The results of the MTT assay correlated well with the observation of the BCA assay (data not shown) in the transfection experiments. Similar results were reported in earlier studies as well (Jiang & Salem, 2012; Sun et al., 2008b).

Furthermore, the compatibility of non-viral vectors with blood indicates their suitability for administration directly into the systemic circulation. The hemolytic behavior of the free polymers was tested as worst case scenario and classified according to the ASTM F756-08 standard (data not shown) (2008). According to this standard, neither free lPEIs nor dex-*g*-lPEIs did show any detectable disturbance of the red blood cell membranes (hemolysis <2%) up to 1 mg mL^{-1}. The observed behavior can be attributed to the low

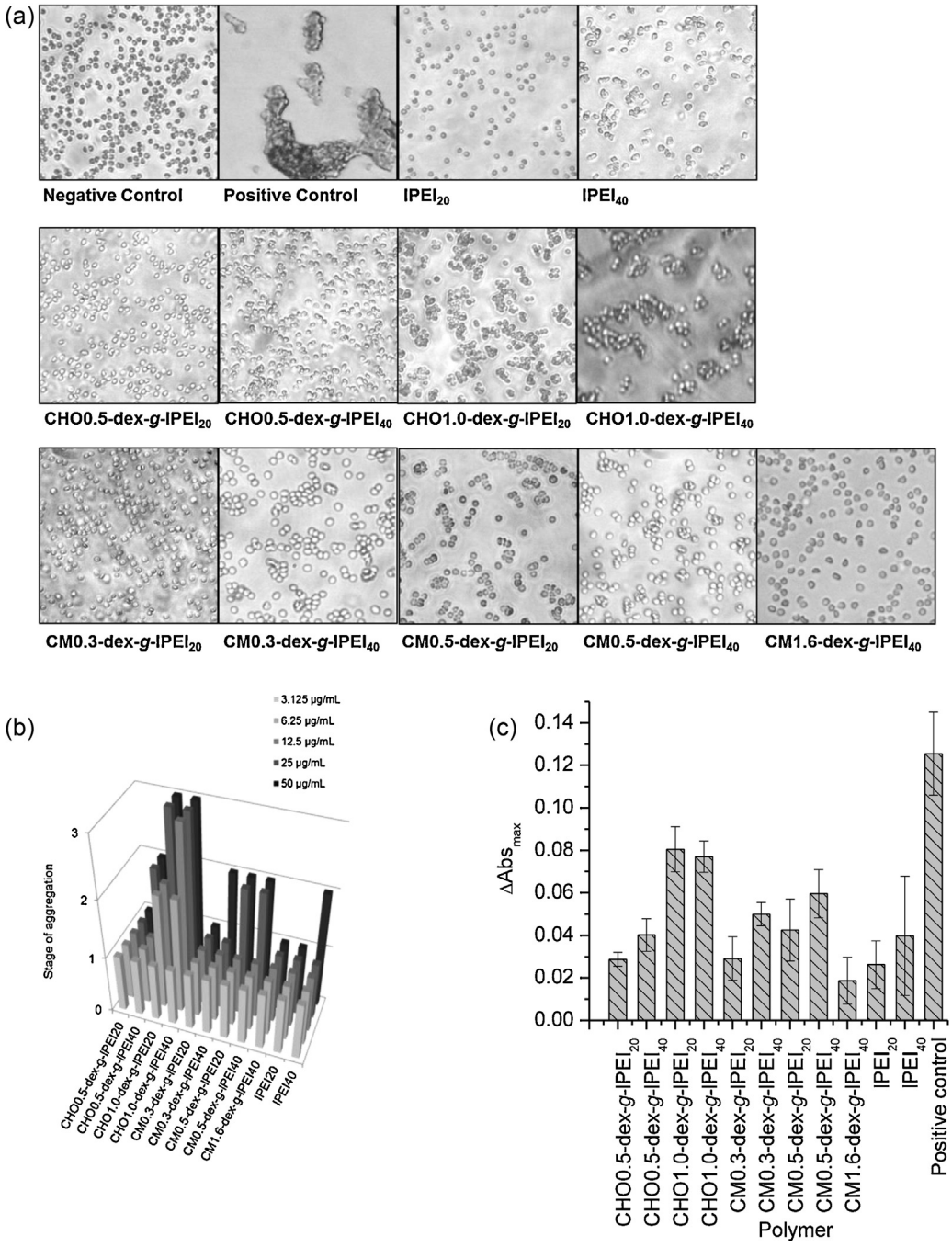

Fig. 5. Aggregation of sheep red blood cells after treatment with free dex-*g*-lPEI and lPEI polymers incubated at 37 °C for 2 h. (a) Representative pictures of microscopic observation at 50 μg mL^{-1} (negative control = PBS; positive control = 15 μg mL^{-1} bPEI 25,000 g mol^{-1}) with magnification 200×. (b) Stages of sheep blood erythrocyte aggregation of dex-*g*-lPEIs and lPEIs at concentrations up to 50 μg mL^{-1}. Classification: 1 = no aggregation of erythrocytes, 2 = moderate aggregation with rouleau formation, 3 = strong aggregation with cluster formation. (c) ΔAbs_{max} of polymers. The RBC aggregation experiments were performed with $n = 2$ and repeated once (mean ± SD).

DS and the low molar mass of the cationic polymers (Moreau, Domurado, Chapon, Vert, & Domurado, 2002). For comparison, dextran itself showed no erythrocyte membrane disturbance up to 16 mg mL^{-1} with 0.2% hemolytic activity (Yang et al., 2012).

To avoid clinical complications like thrombosis and embolism by systemic use of the dextran-based vectors, their potential to aggregate red blood cells was investigated by qualitative light microscopy (Fig. 5a and b) and classified into three stages (Fig. 5b) as well as quantitatively by UV–vis spectroscopy (Fig. 5c). Both methods gave comparable results and displayed a concentration-dependent red blood cell aggregation behavior of the polymers up to 50 μg mL^{-1}. In microscopic experiments, the negative control did not show any signs of cluster formation (stage 1), whereas the positive control (25,000 g mol^{-1} bPEI, 15 μg mL^{-1}) caused the formation of large aggregates (stage 3) as described before (Fig. 5a) (Bauer et al., 2012). Additionally, the ΔAbs_{max} value was introduced, meaning the difference of the reduction in absorbance to the negative control absorbance. In contrast to the positive control ($\Delta Abs_{max} = 0.12$), $lPEI_{20}$ was well tolerated and classified as stage 1 ($\Delta Abs_{max} = 0.026$), whereas an increase in molar mass ($lPEI_{40}$) initiated rouleaux formation only at the highest tested concentration of 50 μg mL^{-1} (stage 2, $\Delta Abs_{max} = 0.04$). The molar mass and concentration dependent effects of PEIs on red blood cell aggregation were described by several authors (Jeon, Yang, Lee, & Kim,

2008; Petersen et al., 2002). Correlated to the increasing number of charges with size, the interactions with negatively charged cell membranes increase as well.

In accordance to the results obtained for the free lPEIs, also for the dex-g-lPEIs an increase of red blood cell aggregation could be observed with higher molar mass of lPEI (Fig. 5). For the **CHO-dex-*g*-lPEIs** erythrocyte aggregation could be observed starting at concentrations of 6.25 and 25 mg mL^{-1} for **CHO$_{1.0}$-dex-*g*-lPEI$_{20}$**, CHO1.0-dex-g-lPEI40, and **CHO$_{0.5}$-dex-*g*-lPEI$_{40}$**, respectively. In contrast, **CHO$_{0.5}$-dex-g-lPEI$_{20}$** did not show any signs of interaction up to the highest tested concentration of 50 μg mL^{-1} (Fig. 5b). Therefore, interactions with negatively charged cell membranes of the red blood cells were found to increase with the molar mass of lPEI; this observation correlated well with the nitrogen content of the **CHO-dex-*g*-lPEIs**. In general, the conjugates synthesized by reductive amination demonstrated a higher red blood cell aggregation potential compared to the modified dextrans prepared by EDC-coupling. **CM$_{0.3}$-dex-*g*-lPEI$_{40}$**, **CM$_{0.5}$-dex-*g*-lPEI$_{20}$**, and **CM$_{0.5}$-dex-*g*-lPEI$_{40}$** reached only stage 2 with maximum Abs$_{max}$ values of 0.06, even at the highest concentration of 50 μg mL^{-1}. Again, for the lPEI40-containing polymers **CM$_{0.3}$-dex-*g*-lPEI$_{40}$** and **CM$_{0.5}$-dex-*g*-lPEI$_{40}$** the aggregation effects were more pronounced than for the lPEI20-based polymers (**CM$_{0.3}$-dex-*g*-lPEI$_{20}$** and **CM$_{0.5}$-dex-*g*-lPEI$_{20}$**). The higher compatibility of the **CM-dex-*g*-lPEIs** compared to the **CHO-dex-*g*-lPEIs** may be ascribed to the polyelectrolyte nature of the **CM-dex-*g*-lPEIs** since they contain both positive and negative charges. This was particularly demonstrated by the polymer **CM$_{1.6}$-dex-*g*-lPEI$_{40}$**, that possesses a higher number of anionic charges and revealed the lowest effects on red blood cells (stage 1 at 50 μg mL^{-1}, Abs$_{max}$ = 0.02). Hence, the high number of anionic charges within the **CM-dex-*g*-lPEI** polymers seems to interfere with the electrostatic interactions between the anionic cell membranes and the cationic polymers resulting in a decreased cell aggregation. De facto, for polyelectrolytes (*e.g.* zwitterionic polymers) a higher resistance to non-specific protein adsorption and blood cell interactions, which lead to a prolonged half life time in blood circulation, has been shown (Jiang & Cao, 2010).

4. Conclusion

With the objective to evaluate the influence of the linking strategy of lPEI to dextran, several dextran-*g*-lPEIs were prepared. For this purpose, different low molar mass lPEIs were synthesized and conjugated to dextran *via* two routes, namely reductive amination and EDC coupling. These linking strategies were already used in the past but mainly lack on a detailed characterization of the resulting molecules and a direct comparison of the different linking strategies (Jiang & Salem, 2012; Sun et al., 2008b). For a detailed comparative study of structure-activity relationships, the content of functional groups (CHO, COOH) within the dextran precursors and the DS with lPEI were varied as well. Subsequently, the final dex-*g*-lPEI samples were characterized in detail and investigated with regard to their physicochemical properties (DNA binding and stabilization, complex size and surface charge), transfection efficiency as well as biocompatibility. The investigations were performed in terms of dependency on the linking strategy, the molar mass of conjugated lPEIs, and the N/P ratio of the formed DNA/dex-*g*-lPEI complexes. Independent from the linking strategy, DS and molar mass of lPEI, it was observed that almost all conjugates formed with DNA were in the range of 100 nm (in water), stable against enzymatic degradation, and revealed a positive surface charge. Differences between the types of conjugation were visible when lPEI was conjugated with CM$_{1.6}$-dex (**CM$_{1.6}$-dex-*g*-lPEI$_{20}$**): The binding capacity was reduced, as well as the stability and the zeta potential, which was attributed to the higher content of COOH groups along the dextran backbone. Moreover, cell viability studies revealed a good cytocompatibility of the resulting dex-*g*-lPEI/DNA complexes with no crucial influence of the synthesis route or the DS and molar mass of lPEI. Instead, a remarkable effect of these parameters was observed regarding transfection efficiency, since the cationic dextrans prepared by EDC coupling showed a more than one order of magnitude increased transgene expression compared to the **CHO-dex-*g*-lPEIs** despite much lower lPEI content. For comparison, free lPEIs formed complexes that showed almost no transgene expression. The additional integration of COOH-groups seems to accomplish a positive to negative charge ratio within the **CM-dex-*g*-lPEI** conjugates that is advantageous for DNA release and transfection efficiency. Their transfection rates were found to be comparable with the positive control 2.5 kDa lPEI. It was also discovered that both polymer series induced higher red blood cell aggregation compared to unconjugated lPEIs, with **CM-dex-*g*-lPEI** showing a lower erythrocyte aggregation activity than **CHO-dex-*g*-lPEI**. This was again ascribed to the polyelectrolyte nature of the **CM-dex-*g*-lPEI**.

In conclusion, the variation of the linking strategy of cationic polymers to dextran affects the biological properties significantly, while the physicochemical properties were only marginally affected. The EDC coupling was more suitable as linking strategy compared to the polymers obtained by reductive amination, since the conjugates showed improved hemocompatibility and enhanced performance in the transfection experiments.

Acknowledgements

Financial support from the Thuringian Ministry for Education, Science and Culture (grant no. B514-09051, NanoConSens) and from the Carl-Zeiss Foundation (JCSM Strukturantrag) is gratefully acknowledged. The authors also thank Angela Herre, Ramona Brabetz and Maxi Prange for their excellent laboratory assistance.

Appendix A. Supplementary data

Supplementary material related to this article can be found, in the online version, at http://dx.doi.org/10.1016/j.carbpol.2014.07.048.

References

Abdullah, S., Wendy-Yeo, W. Y., Hosseinkhani, H., Hosseinkhani, M., Masrawa, E., Ramasamy, R., Rosli, R., Rahman, S. A., & Domb, A. J. (2010). Gene transfer into the lung by nanoparticle dextran-spermine/plasmid DNA complexes. *Journal Biomedical Biotechnology*, *2010*, 284840.

Altuntaş, E., Knop, K., Tauhardt, L., Kempe, K., Crecelius, A. C., Jäger, M., Hager, M. D., & Schubert, U. S. (2012). Tandem mass spectrometry of poly(ethylene imine)s by electrospray ionization (ESI) and matrix-assisted laser desorption/ionization (MALDI). *Journal of Mass Spectrometry*, *47*(1), 105–114.

ASTM. (2008). *Standard practice for assessment of hemolytic properties of materials. Annual book of ASTM standards* (vol. 13) Philadelphia, PA: ASTM. ASTM F756-13

Azzam, T., Eliyahu, H., Shapira, L., Linial, M., Barenholz, Y., & Domb, A. J. (2002). Polysaccharide-oligoamine based conjugates for gene delivery. *Journal of Medicinal Chemistry*, *45*(9), 1817–1824.

Bauer, M., Lautenschlaeger, C., Kempe, K., Tauhardt, L., Schubert, U. S., & Fischer, D. (2012). Poly(2-ethyl-2-oxazoline) as alternative for the stealth polymer poly(ethylene glycol): Comparison of in vitro cytotoxicity and hemocompatibility. *Macromolecular Bioscience*, *12*(7), 986–998.

Breunig, M., Lungwitz, U., Liebl, R., Fontanari, C., Klar, J., Kurtz, A., Blunk, T., & Goepferich, A. (2005). Gene delivery with low molecular weight linear polyethylenimines. *Journal of Gene Medicine*, *7*(10), 1287–1298.

Cavallaro, G., Scirè, S., Licciardi, M., Ogris, M., Wagner, E., & Giammona, G. (2008). Polyhydroxyethylaspartamide-spermine copolymers: Efficient vectors for gene delivery. *Journal of Controlled Release*, *131*(1), 54–63.

Chu, M., Dong, C., Zhu, H., Cai, X., Dong, H., Ren, T., Su, J., & Li, Y. (2013). Biocompatible polyethylenimine-graft-dextran catiomer for highly efficient gene delivery assisted by a nuclear targeting ligand. *Polymer Chemistry*, *4*(8), 2528–2539.

Cohen, J. L., Schubert, S., Wich, P. R., Cui, L., Cohen, J. A., Mynar, J. L., & Frećhet, J. M. J. (2011). Acid-degradable cationic dextran particles for the delivery of siRNA therapeutics. *Bioconjugate Chemistry*, *22*(6), 1056–1065.

Eshita, Y., Higashihara, J., Onishi, M., Mizuno, M., Yoshida, J., Takasaki, T., Kubota, N., & Onishi, Y. (2009). Mechanism of introduction of exogenous genes into cultured cells using DEAE-dextran-MMA graft copolymer as non-viral gene carrier. *Molecules*, *14*(7), 2669–2683.

Fischer, D., Dautzenberg, H., Kunath, K., & Kissel, T. (2004). Poly(diallyldimethylammonium chlorides) and their *N*-methyl-*N*-vinylacetamide copolymer-based DNA-polyplexes: Role of molecular weight and charge density in complex formation, stability, and in vitro activity. *International Journal of Pharmaceutics*, *280*(1–2), 253–269.

Gebhart, C. L., Sriadibhatla, S., Vinogradov, S., Lemieux, P., Alakhov, V., & Kabanov, A. V. (2002). Design and formulation of polyplexes based on pluronic-polyethyleneimine conjugates for gene transfer. *Bioconjugate Chemistry*, *13*(5), 937–944.

Godbey, W. T., Barry, M. A., Saggau, P., Wu, K. K., & Mikos, A. G. (2000). Poly(ethylenimine)-mediated transfection: A new paradigm for gene delivery. *Journal of Biomedical Materials Research*, *51*(3), 321–328.

Grund, S., Bauer, M., & Fischer, D. (2011). Polymers in drug delivery—State of the art and future trends. *Advanced Engineering Materials*, *13*(3), B61–B87.

Heinze, T., Erler, U., Nehls, I., & Klemm, D. (1994). Determination of the substituent pattern of heterogeneously and homogeneously synthesized carboxymethyl cellulose by using high-performance liquid chromatography. *Angewandte Makromolekulare Chemie*, *215*(1), 93–106.

Heinze, T., Liebert, T., Heublein, B., & Hornig, S. (2006). Functional polymers based on dextran. *Advances in Polymer Science*, *205*, 199–291.

International Organization for Standardization/ANSI. (2009). Biological evaluation of medical devices Part 5: Tests for in vitro cytotoxicity. In *ISO 10993-5* (2nd ed.). Geneva, Switzerland: International Organization for Standardization/ANSI.

Jeanes, A., & Wilham, C. A. (1950). Periodate oxidation of dextran. *Journal of the American Chemical Society*, *72*(6), 2655–2657.

Jeon, O., Yang, H. S., Lee, T.-J., & Kim, B.-S. (2008). Heparin-conjugated polyethylenimine for gene delivery. *Journal of Controlled Release*, *132*(3), 236–242.

Jiang, D., & Salem, A. K. (2012). Optimized dextran-polyethylenimine conjugates are efficient non-viral vectors with reduced cytotoxicity when used in serum containing environments. *International Journal of Pharmaceutics*, *427*(1), 71–79.

Jiang, S., & Cao, Z. (2010). Ultralow-fouling, functionalizable, and hydrolyzable zwitterionic materials and their derivatives for biological applications. *Advanced Materials*, *22*(9), 920–932.

Kent, P. W. (1949). Periodate oxidation in the study of the structure of dextrans. *Science*, *110*(2869), 689–690.

Knop, K., Hoogenboom, R., Fischer, D., & Schubert, U. S. (2010). Poly(ethylene glycol) in drug delivery: Pros and cons as well as potential alternatives. *Angewandte Chemie International Edition*, *49*(36), 6288–6308.

Liebert T., Heinze T. (1998). Induced phase separation: A new synthesis concept in cellulose chemistry, In: Cellulose derivatives: Synthesis, characterization and nansotructures. ACS Symposium Series No. 688, W.G. Glaser and T. Heinze (eds.), American Chemical Society, Washington DC, pp. 1-72.

Lungwitz, U., Breunig, M., Liebl, R., Blunk, T., & Goepferich, A. (2008). Methoxy poly(ethylene glycol)—Low molecular weight linear polyethylenimine-derived copolymers enable polyplex shielding. *European Journal of Pharmaceutics and Biopharmaceutics*, *69*(1), 134–148.

Maruyama, A., Watanabe, H., Ferdous, A., Katoh, M., Ishihara, T., & Akaike, T. (1998). Characterization of interpolyelectrolyte complexes between double-stranded DNA and polylysine comb-type copolymers having hydrophilic side chains. *Bioconjugate Chemistry*, *9*(2), 292–299.

Mehvar, R. (2000). Dextrans for targeted and sustained delivery of therapeutic and imaging agents. *Journal of Controlled Release*, *69*(1), 1–25.

Moreau, E., Domurado, M., Chapon, P., Vert, M., & Domurado, D. (2002). Biocompatibility of polycations: In vitro agglutination and lysis of red blood cells and in vivo toxicity. *Journal of Drug Targeting*, *10*(2), 161–173.

Ogris, M., Brunner, S., Schuller, S., Kircheis, R., & Wagner, E. (1999). PEGylated DNA/transferrin-PEI complexes: Reduced interaction with blood components, extended circulation in blood and potential for systemic gene delivery. *Gene Therapy*, *6*(4), 595–605.

Ogris, M., Steinlein, P., Kursa, M., Mechtler, K., Kircheis, R., & Wagner, E. (1998). The size of DNA/transferrin-PEI complexes is an important factor for gene expression in cultured cells. *Gene Therapy*, *5*(10), 1425–1433.

Ogris, M., Walker, G., Blessing, T., Kircheis, R., Wolschek, M., & Wagner, E. (2003). Tumor-targeted gene therapy: strategies for the preparation of ligand-polyethylene glycol-polyethylenimine/DNA complexes. *Journal of Controlled Release*, *91*(1–2), 173–181 (Proceedings of the Second International Symposium on Tumor Targeted Delivery Systems).

Park, M. R., Han, K. O., Han, I. K., Cho, M. H., Nah, J. W., Choi, Y. J., & Cho, C. S. (2005). Degradable polyethylenimine-alt-poly(ethylene glycol) copolymers as novel gene carriers. *Journal of Controlled Release*, *105*(3), 367–380.

Petersen, H., Fechner, P. M., Martin, A. L., Kunath, K., Stolnik, S., Roberts, C. J., Fischer, D., Davies, M. C., & Kissel, T. (2002). Polyethylenimine-graft-poly(ethylene glycol) copolymers: Influence of copolymer block structure on DNA complexation and biological activities as gene delivery system. *Bioconjugate Chemistry*, *13*(4), 845–854.

Rankin, J. C., & Jeanes, A. (1954). Evaluation of the periodate oxidation method for structural analysis of dextrans. *Journal of the American Chemical Society*, *76*(17), 4435–4441.

Rinkenauer, A. C., Vollrath, A., Schallon, A., Tauhardt, L., Kempe, K., Schubert, S., Fischer, D., & Schubert, U. S. (2013). Parallel high-throughput screening of polymer vectors for nonviral gene delivery: Evaluation of structure–property relationships of transfection. *ACS Combinatorial Science*, *15*(9), 475–482.

Sun, K., Wang, J., Zhang, J., Hua, M., Liu, C., & Chen, T. (2011). Dextran-*g*-PEI nanoparticles as a carrier for co-delivery of adriamycin and plasmid into osteosarcoma cells. *International Journal of Biological Macromolecules*, *49*(2), 173–180.

Sun, Y.-X., Xiao, W., Cheng, S.-X., Zhang, X.-Z., & Zhuo, R.-X. (2008). Synthesis of (dex-HMDI)-*g*-PEIs as effective and low cytotoxic nonviral gene vectors. *Journal of Controlled Release*, *128*(2), 171–178.

Sun, Y.-X., Zhang, X.-Z., Cheng, H., Cheng, S.-X., & Zhuo, R.-X. (2008). A low-toxic and efficient gene vector: Carboxymethyl dextran-graft-polyethylenimine. *Journal of Biomedical Materials Research A*, *84A*(4), 1102–1110.

Tauhardt, L., Kempe, K., Knop, K., Altuntaş, E., Jäger, M., Schubert, S., Fischer, D., & Schubert, U. S. (2011). Linear polyethyleneimine: Optimized synthesis and characterization—On the way to "Pharmagrade" batches. *Macromolecular Chemistry and Physics*, *212*(17), 1918–1924.

Thomas, J. J., Rekha, M. R., & Sharma, C. P. (2010a). Dextran-glycidyltrimethylammonium chloride conjugate/DNA nanoplex: A potential non-viral and haemocompatible gene delivery system. *International Journal of Pharmaceutics*, *389*(1–2), 195–206.

Thomas, J. J., Rekha, M. R., & Sharma, C. P. (2010b). Dextran-protamine polycation: An efficient nonviral and haemocompatible gene delivery system. *Colloids and Surfaces B: Biointerfaces*, *81*(1), 195–205.

Thomas, M., Ge, Q., Lu, J. J., Chen, J., & Klibanov, A. (2005). Cross-linked small polyethylenimines: While still nontoxic, deliver DNA efficiently to mammalian cells in vitro and in vivo. *Pharmaceutical Research*, *22*(3), 373–380.

Tripathi, S. K., Goyal, R., & Gupta, K. C. (2011). Surface modification of crosslinked dextran nanoparticles influences transfection efficiency of dextran-polyethylenimine nanocomposites. *Soft Matter*, *7*(24), 11360–11371.

Tseng, W.-C., Fang, T.-Y., Su, L.-Y., & Tang, C.-H. (2005). Dependence of transgene expression and the relative buffering capacity of dextran-grafted polyethylenimine. *Molecular Pharmaceutics*, *2*(3), 224–232.

Tseng, W.-C., & Jong, C.-M. (2003). Improved stability of polycationic vector by dextran-grafted branched polyethylenimine. *Biomacromolecules*, *4*(5), 1277–1284.

Tseng, W.-C., Tang, C.-H., & Fang, T.-Y. (2004). The role of dextran conjugation in transfection mediated by dextran-grafted polyethylenimine. *Journal of Gene Medicine*, *6*(8), 895–905.

van Gaal, E. V. B., van Eijk, R., Oosting, R. S., Kok, R. J., Hennink, W. E., Crommelin, D. J. A., & Mastrobattista, E. (2011). How to screen non-viral gene delivery systems in vitro? *Journal of Controlled Release*, *154*(3), 218–232.

Vandoorne, F., Bruneel, D., Vercauteren, R., & Schacht, E. (1991). New approach to dextran derivatives containing primary amino functions. *Makromolekulare Chemie*, *192*(3), 673–677.

Varshosaz, J. (2012). Dextran conjugates in drug delivery. *Expert Opinion on Drug Discovery*, *9*(5), 509–523.

Vlugt-Wensink, K. D. F., Vrueh, R., Gresnigt, M. G., Hoogerbrugge, C. M., Buul-Offers, S. C., Leede, L. G. J., Sterkman, L. G. W., Crommelin, D. J. A., Hennink, W. E., & Verrijk, R. (2007). Preclinical and clinical in vitro in vivo correlation of an hGH dextran microsphere formulation. *Pharmaceutical Research*, *24*(12), 2239–2248.

Wotschadlo, J., Liebert, T., Heinze, T., Wagner, K., Schnabelrauch, M., Dutz, S., Mueller, R., Steiniger, F., Schwalbe, M., Kroll, T. C., Hoeffken, K., Buske, N., & Clement, J. H. (2009). Magnetic nanoparticles coated with carboxymethylated polysaccharide shells—Interaction with human cells. *Journal of Magnetism and Magnetic Materials*, *321*(10), 1469–1473.

Xiao, W., Sun, Y.-X., Cheng, H., Zeng, X., Zhang, X.-Z., & Zhuo, R.-X. (2010). Inhibition of enhanced green fluorescent protein expression by (dextran-hexamethylenediisocyanate)-*g*-polyethylenimine/siRNA complexes. *Journal of Microencapsulation*, *27*(5), 447–452.

Yang, J., Liu, Y., Wang, H., Liu, L., Wang, W., Wang, C., Wang, Q., & Liu, W. (2012). The biocompatibility of fatty acid modified dextran-agmatine bioconjugate gene delivery vector. *Biomaterials*, *33*(2), 604–613.

Yu, J.-H., Quan, J.-S., Kwon, J.-T., Xu, C.-X., Sun, B., Jiang, H.-L., Nah, J.-W., Kim, E.-M., Jeong, H.-J., Cho, M.-H., & Cho, C.-S. (2009). Fabrication of a novel core-shell gene delivery system based on a brush-like polycation of α, β-poly (L-aspartate-graft-PEI). *Pharmaceutical Research*, *26*(9), 2152–2163.

Zhao, H., & Heindel, N. D. (1991). Determination of degree of substitution of formyl groups in polyaldehyde dextran by the hydroxylamine hydrochloride method. *Pharmaceutical Research*, *8*(3), 400–402.